proceedings

MDPI

Proceedings

A BODIPY-Based Fluorescent Sensor for Amino Acids Bearing Thiol †

Edurne Avellanal-Zaḅalla [1], Ágata Ramos-Torres [2], Alejandro Prieto-Castañeda [2], Fernando García-Garrido [2], Jorge Bañuelos [1,*], Antonia R. Agarrabeitia [2] and María J. Ortiz [2,*]

[1] Dpto Química Física, Facultad de Ciencia y Tecnología, Universidad del País Vasco (UPV/EHU), Aptdo 644, 48080 Bilbao, Spain; edurne.avellanal@ehu.es

[2] Dpto Química Orgánica I, Facultad de Ciencias Químicas, Universidad Complutense de Madrid, Ciudad Universitaria s/n, 28040 Madrid, Spain; agatei@hotmail.com (Á.R.-T.); alprieto@ucm.es (A.P.-C.); fernanga@ucm.es (F.G.-G.); agarrabe@quim.ucm.es (A.R.A.)

* Correspondence: jorge.banuelos@ehu.es (J.B.); mjortiz@quim.ucm.es (M.J.O.)

† Presented at the 23rd International Electronic Conference on Synthetic Organic Chemistry, 15 November–15 December 2019; Available online: https://ecsoc-23.sciforum.net/.

Published: 14 November 2019

Abstract: Herein, we describe the synthetic route to access a red-emitting BODIPY from its α-diformylated precursor. The photophysical signatures of this dye are sensitive to the presence of thiol-containing amino acids (like cysteine, homocysteine, and glutathione) in the surrounding environment. This sensor provides up to three detection channels to monitor and quantify these biomolecules, even at low concentrations (down to micromolar). Moreover, owing to the pronounced splitting of the spectral band profile induced by these amino acids, the detection can be visualized following just the evolution of the fluorescence color by the naked eye.

Keywords: dye chemistry; fluorescent sensors; BODIPY; amino acids; Wittig reaction

1. Introduction

The molecular design of fluorescent sensors to monitor and quantify the presence of biomolecules in physiological media is actually a hot research topic, owing to the key role of some of these biomolecules in biochemical events and diseases [1,2]. In this regard, the detection of amino acids (AA) is in the spotlight and, in particular, there is great interest in the development of effective and sensitive sensors to detect cysteine (CYS), homocysteine (HCYS) and glutathione (GSH) owing to their biological role [3–5]. These thiol-containing AAs are involved in the growth of cells and tissues, and in the cellular defense against toxins. Moreover, alterations in the local concentration of these AA are related to different diseases, from cancer to Alzheimer and a wide assortment of cardiovascular illnesses [6,7]. Therefore, suitable detection and quantification of these thiol-based AA in the biological media would allow an early diagnosis of some diseases, as well as provide a deeper insight into the biochemical mechanism of such illnesses, providing valuable information for their treatment.

Among the available strategies for sensing, fluorescent chemosensors represent one of the best choices [8–10]. Fluorescence is a useful tool to translate straightforwardly chemical information, like concentration of AA, into analytical information, just following the emission signal at real time, in situ and via non-invasive methods. To this aim, molecular engineering is a key issue because the fluorophore should be functionalized with a recognition site for the target analyte. Overall, there are two main approaches to design sensors and report the binding of the analyte via the fluorescence signal, the on-off switches and the ratiometric sensors. In the former case, the receptor of the analyte induces a drastic quenching (usually via activation of photoinduced electron transfer processes) of

the emission from the chromohore (off state). Upon binding of the analyte to the receptor, such quenching pathway is suppressed, and the fluorescence signal is suddenly recovered (on state). These switches are usually applied for the detection of ions. On the other hand, in the ratiometric sensors, the receptor induces a drastic change in the spectral signatures (for instance spectral shifts) of the fluorohore. Once the analyte interacts with the recognition site of the chomophore the above-mentioned alteration is modulated, leading to the growing and/or decrease of the absorption and/or emission band. Thus, different spectral windows can be used to monitor and quantify the presence of the analyte.

With regard, to the emitting unit of the chemosensor different dyes have been tested, but those known as boron-dipyrromethenes (BODIPY) have gained recognition owing to their outstanding performance [11–13]. This chromophore is chemically robust, stable under hard irradiation doses and shows excellent photophysical properties [14–16]. Nevertheless, likely its main advantage is the impressive chemical versatility of its boron-dipyrrin backbone, which allows a fine control and tailoring of the photophysical signatures [17,18]. Therefore, a wide assortment of chemical modifications can be applied at the chromophore leading to a vast battery of available functional group [19,20]. Bearing in mind that to design sensors, a suitable receptor for the target analyte should be chemically added to the fluorophore, BODIPY dye is an ideal molecular scaffold because it displays stable and bright emission, which can be modulated, and at the same time it can be easily post-functionalized with a myriad of moieties acting as recognition sites.

Against this background, we have designed and synthesized the ratiometric chemosensor **1**, based on BODIPY (Scheme 1), for the sensing of the aforementioned AA bearing thiol. The chromophoric core of this fluorophore has been decorated with unsaturated esters at both α-pirrolic positions. This functionalization has a dual purpose. On the one hand, it induces a pronounced bathochromic shift of the spectral bands towards the red-edge of the visible, which enhances the penetration of the light into tissues avoiding interference of the surrounding bioenvironment. On the other hand, it acts as the recognition site for CYS, HCYS and GSH, since the double bond and the carbonyl groups are able to react with the nucleophilic amine or thiol groups of these AAs. Hereafter, we describe the synthetic route and the spectroscopic changes induced by the tested AA for sensing.

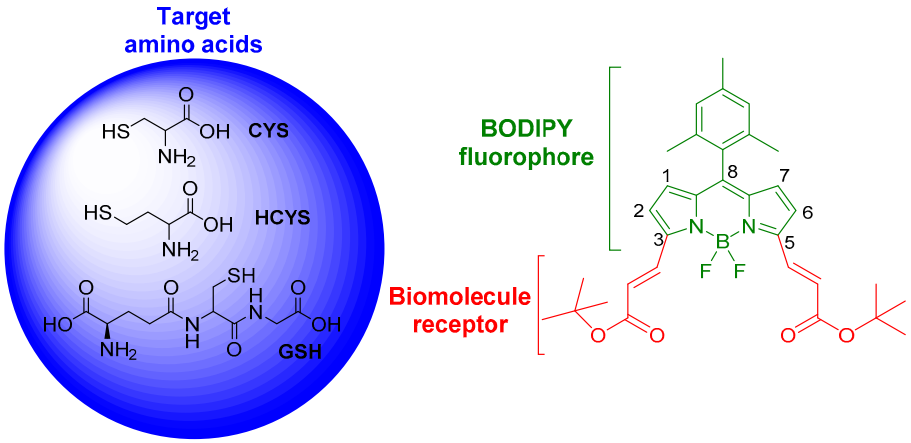

Scheme 1. Molecular structure of the BODIPY based fluorescent chemosensor **1** for thiol-bearing AA.

2. Results and Discussion

The BODIPY based sensor is attained by an oxidation with pyridinium chlorochromate (PCC) of 8-mesityl-3,5-dimethylBODIPY (**2**) [21,22], giving rise to α-formyl precursor **3** (Scheme 2). A new oxidation reaction with PCC affords the α,α-diformylated derivative **4**. The access to this intermediate is the key step since the aldehyde is very versatile owing to its reactivity. The synthetic protocol to attain this 3,5-diformylBODIPY with moderate yields, via oxidation with PCC at soft conditions, has been reported previously [23]. Afterwards, such formyls can be easily and efficiently converted to the α, β-unsaturated diesters **1** via the Wittig reaction (Scheme 2) [23].

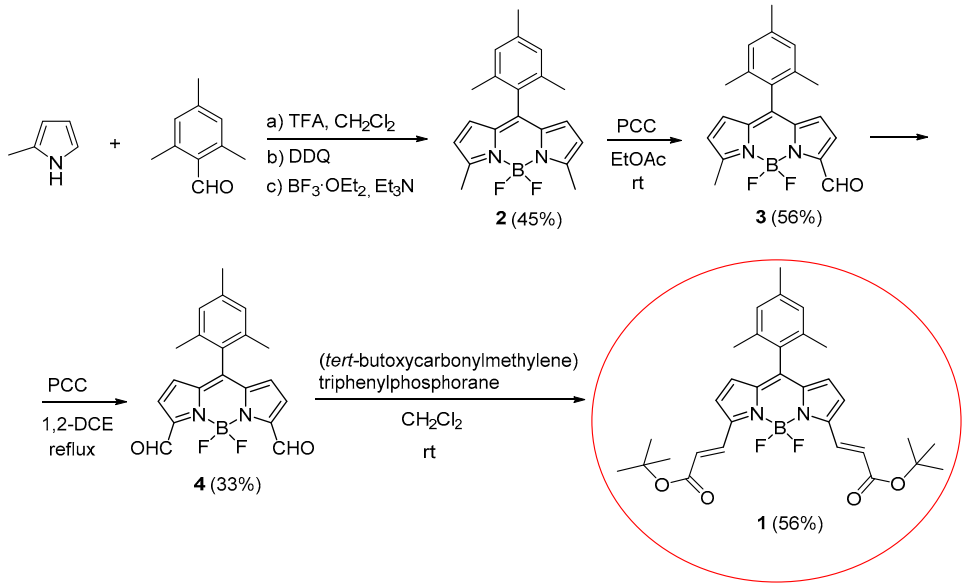

Scheme 2. Synthesis of 3,5-Bis(3-*tert*-butoxy-3-oxoprop-1-en-1-yl) BODIPY.

The spectroscopic properties of the sensor **1** are ruled by the resonant interaction between the unsaturated esters and the dipyrrine core. Indeed, the theoretical simulations envisage that the localized π-system is extended through such aromatic arms at α-pyrrolic positions (see the computed contour maps of the frontier orbitals involved in the transition in Figure 1). As consequence, the spectral bands are shifted towards the red-edge of the visible spectral region (Figure 1). In particular, the main absorption bands is placed at the orange region with a molar coefficient of 59,000 M^{-1} cm^{-1}, whereas the corresponding fluorescence band locates in the beginning of the red, with a remarkable fluorescence efficiency of 62% and a lifetime of 5.42 ns.

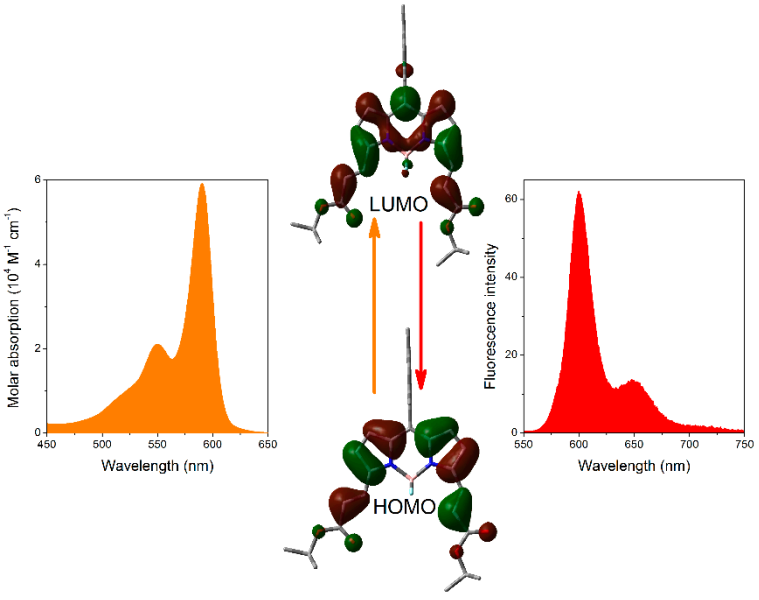

Figure 1. Absorption and fluorescence spectra of the chemosensor (dye concentration 2 μM) in ethanol, together with the computed frontier orbitals (Highest Occupied Molecular Orbital, HOMO, and Lowest Unoccupied Molecular Orbital, LUMO) involved in such electronic transitions (b3lyp/6-311+g*) simulating also the ethanol solvent (Polarizable Continuum Model, PCM).

The presence of the tested AA induces pronounced changes in the absorption and fluorescence spectral profiles (Figures 2 and 3). Indeed, the bands are clearly splitted into three bands, whose relative intensity markedly depends on the concentration of AA in the media. As a common rule, the

AA provokes a loss of the long-wavelength absorption (590 nm) and a concomitance increase of the two short-wavelengths absorptions (550 nm and 515 nm). Similar trends are observed in the fluorescence spectra; the expected emission at 600 nm progressively decrease while the new emissions at 560 nm and 525 nm increase. Nonetheless, the sensitivity of the fluorescence signatures is more marked than in absorption (Figure 3 vs. Figure 2). Even at a low concentration of AA (down to micromolar), an evident increase of the fluorescence at 560 nm is recorded. Higher AA concentrations are required to clearly see the growing of the emission at 525 nm. These spectral evolutions are the same regardless of the tested AA, albeit the chemosensor is less sensitive to GSH than to CYS and HCYS.

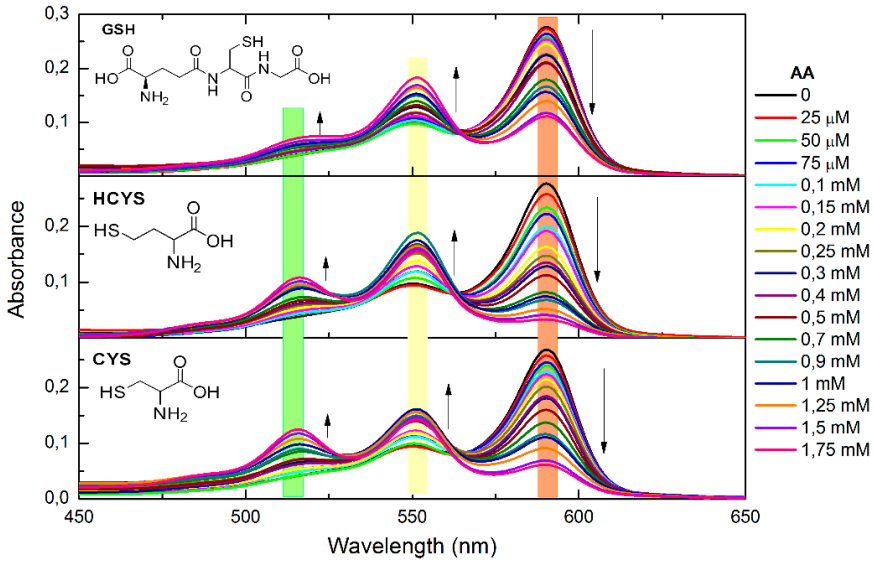

Figure 2. Absorption spectra of the chemosensor **1** (dye concentration 2 μM) at different concentrations of CYS, HCYS and GSH in ethanol/HEPES (1:1) mixtures to mimic the physiological media.

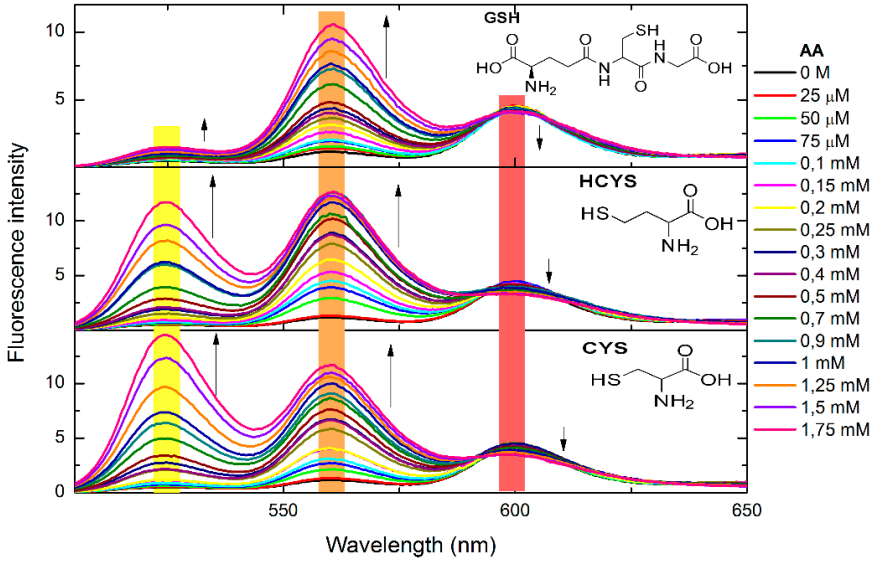

Figure 3. Fluorescence spectra of the chemosensor **1** (dye concentration 2 μM) at different concentrations of CYS, HCYS and GSH in ethanol/HEPES (1:1) mixtures to mimic the physiological media.

Therefore, the presence of these AA can be straightforwardly monitored just following the fluorescence response. Moreover, the BODIPY based sensor **1** behaves as a highly sensitive ratiometric indicator thanks to the growing/decrease of the emission bands, providing up to three

detection channels to quantify the concentration of AA in the media. To highlight such versatility to visualize the AA, in Figure 4 we have plotted the evolution of the fluorescence intensity at the selected wavelengths of each channel. The noticeable increase of the emission at 560 nm (orange emission) and 525 nm (yellow emission) are the most effective channels to recognize the presence of the AA. Moreover, such detection can be easily done qualitatively just by the naked eye owing to the discernable change of the emission color, at lower AA concentration from red to orange, and at higher concentrations from orange to yellow (Figure 4).

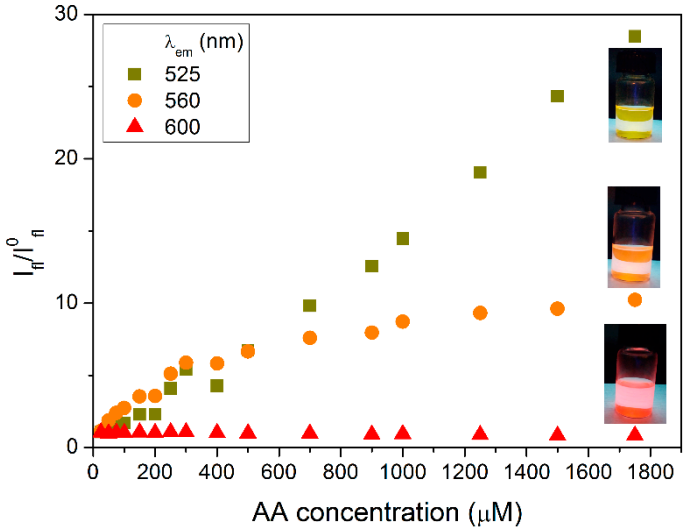

Figure 4. Ratio between the fluorescence intensity with AA in the media and without it at different concentrations of CYS, as representative AA, and at the three selected detection channels; 525 nm, 560 nm, and 600 nm.

The underlying mechanism in the sensing should be related with a chemical reaction between the AA (involving the electron donor amino group and likely the more nucleophilic thiol) and the unsaturated ester of the chromophore (through the vinyl and carbonyl as reactive sites). We hypothesize that such an interaction decreases the extension of the conjugated chromophoric π-system leading to the recorded shorter wavelength absorptions and emission. In other words, the selective interaction of the AA with the carbonyl would reduce the extension of the π-system of the BODIPY core just to both vinyls, leading to the absorption and fluorescence band at 550 nm and 560 nm, respectively. Further interaction of the AA with the vinyl would limit the π-system to the dipyrrin core, this being responsible for the absorption and emission at 515 nm and 525 nm, respectively. Such assignment is backed up by the typical absorption and emission wavelengths of the simplest BODIPY, which match those of the shortest wavelength absorption and fluorescence in the sensor (515 nm and 525 nm, respectively). Moreover, a bathochromic shift of 35 nm by the attachment of α-pyrrolic vinyls is also consistent to explain the absorption and fluorescence bands at 550 nm and 560 nm.

3. Conclusions

We have successfully designed a ratiometric chemosensor based on BODIPY to detect CYS, HCYs, and GSH. The added unsaturated ester functionalization acts as recognition site for the AA and shift the spectral bands of the luminophore. The presence of AA, even at low concentrations (micromolar) in the surrounding environment, modulates such shift leading to the recording of splitted bands, mainly in fluorescence. Therefore, this highly sensitive sensor provides up to three channels to quantify the concentration of AA, since the emission color switches from red to orange and to yellow as the concentration of AA increase.

Author Contributions: E.A.-Z. conducted the photophysical measurements; Á.R.-T. and A.P.-C. synthesized the sensor; F.G.-G. carried out the structural and chemical characterization of the compound; J.B. wrote the original

draft and supervised the spectroscopic study, A.R.A. supervised the organic synthesis; M.J.O. designed the sensor and reviewed the writing. All authors have read and agree to the published version of the manuscript.

Funding: This research was funded by Spanish Ministerio de Economía y Competitividad and Gobierno Vasco, grant number MAT2017-83856-C3-2-P and 3-P, and IT912-16, respectively.

Acknowledgments: E.A.-Z. thanks Gobierno Vasco for a predoctoral fellowship. Á.R.-T., A.P.-C. and F.G.-G. thank Comunidad de Madrid, for a postdoctoral contract and two research assistant contracts respectively.

Conflicts of Interest: The authors declare no conflict of interest.

References

1. Biju, V. Chemical modifications and bioconjugate reactions of nanomaterials for sensing, imaging, drug delivery and therapy. *Chem. Soc. Rev*. **2014**, *43*, 744–764, doi:10.1039/c3cs60273g.
2. Ulrich, S.; Dumy, P.; Boturyn, D.; Renaudet, O. Engineering of biomolecules for sensing and imaging applications. *J. Drug Deliv. Sci. Technol*. **2013**, *23*, 5–15, doi:10.1016/S1773-2247(13)50001-3.
3. Chen, X.; Zhou, Y.; Peng. X.; Yoon, J. Fluorescent and colorimetric probes for detection of thiols. *Chem. Soc. Rev*. **2010**, *39*, 2120–2135, doi:10.1039/b925092a.
4. Li, X.; Gao, X.; Shi, W.; Ma. H. Design strategies for water-soluble small molecular chromogenic and fluorogenic probes. *Chem. Rev*. **2014**, *114*, 590–659, doi:10.1021/cr300508p.
5. Tang, Y.; Lee, D.; Wang, J.; Li, G.; Yu, J.; Lin, W.; Yoon, J. Development of fluorescent probes based on protection-deprotection of the key functional groups for biological imaging. *Chem. Soc. Rev*. **2015**, *44*, 5003–5015, doi:10.1039/c5cs00103j.
6. Seshadri, S.; Beiser, A.; Selhub, J.; Jacques, P.F.; Rosenberg, I.H.; D'Agostino, R.B.; Wilson, P.W.F.; Wolf, P.A. Plasma homocysteine as a risk factor for dementia and Alzheimer's disease. *N. Engl. J. Med*. **2002**, *346*, 476–483, doi:10.1056/NEJMoa011613.
7. Sibrian-Vazquez, M.; Escobedo, J.O.; Lim, S.; Samoei, G.K.; Strongin, R.M. Homocystamides promote free-radical and oxidative damage to proteins. *Proc. Natl. Acad. Sci. USA* **2010**, *107*, 551–554, doi:10.1073/pnas.0909737107.
8. Prasanna de Silva, A.; Gunaratne, H.Q.N.; Gunnlaugsson, T.; Huxley, A.J.M.; McCoy, C.P.; Rademacher, J.T.; Rice, T.E. Signaling recognition events with fluorescent sensors and switches. *Chem. Rev*. **1997**, *97*, 1515–1566, doi:10.1021/cr960386p.
9. Rurack, K.; Resch-Genger, U. Rigidization, preorientation and electronic decoupling—The 'magic triangle' for the design of highly efficient fluorescent sensors and switches. *Chem. Soc. Rev*. **2002**, *31*, 116–127, doi:10.1039/b100604p.
10. Wu, D.; Sedgwick, A.C.; Gunnlaugsson, T.; Akkaya, E.U.; Yoon, J.; James, T.D. Fluorescent chemosensors: The past, present and future. *Chem. Soc. Rev*. **2017**, *46*, 7105–7123, doi:10.1039/c7cs00240h.
11. Niu, L.-Y.; Guan, Y.-S.; Chen, Y.-Z.; Wu, L.-Z.; Tung, C.-H.; Yang, Q-Z. BODIPY-based ratiometric fluorescent sensor for highly selective detection of glutathione over cysteine and homocysteine. *J. Am. Chem. Soc*. **2012**, *134*, 18928–18931, doi:10.1021/ja309079f.
12. Boens, N.; Leen, V.; Dehaen, W. Fluorescent indicators based on BODIPY. *Chem. Soc. Rev*. **2012**, *41*, 1130–1172, doi:10.1039/c1cs15132k.
13. Kolemen, S.; Akkaya, E.U. Reaction-based BODIPY probes for selective bio-imaging. *Coord. Chem. Rev*. **2018**, *354*, 121–134, doi:10.1016/jccr.2017.06.021.
14. Loudet, A.; Burgess, K. BODIPY dyes and their derivatives: Syntheses and spectroscopic properties. *Chem. Rev*. **2007**, *107*, 4891–4932, doi:10.1021/cr078381n.
15. Benniston, A.C.; Copley, G. Lighting the way ahead with boron dipyrromethene (Bodipy) dyes. *Phys. Chem. Chem. Phys*. **2009**, *11*, 4124–4131, doi:10.1039/b901383k.
16. Bañuelos, J. BODIPY dye, the most versatile fluorophore ever? *Chem. Rec*. **2016**, *16*, 335–348, doi:10.1002/tcr.201500238.
17. Ulrich, G.; Ziessel, R.; Harriman, A. The chemistry of fluorescent BODIPY dyes: Versatility unsurpassed. *Angew. Chem. Int. Ed.* **2008**, *47*, 1184–1201, doi:10.1002/anie.200702070.
18. Clarke, R.G.; Hall, M.J. Recent developments in the synthesis of the BODIPY dyes. *Adv. Heterocycl. Chem.* **2019**, *128*, 181–261, doi:10.1016/bsaihch.2018.12.001.
19. Boens, N.; Verbelen, B.; Dehaen, W. Postfunctionalization of the BODIPY core: Synthesis and spectroscopy. *Eur. J. Org. Chem*. **2015**, 6577–6595, doi:10.1002/ejoc.201500682.

20. Boens, N.; Verbelen, B.; Ortiz, M.J.; Jiao, J.; Dehaen, W. Synthesis of BODIPY dyes through postfunctionalization of the boron dipyrromethene core. *Coord. Chem. Rev.* **2019**, *399*, 213024, doi:10.1016/jccr.2019.213024.
21. Kusaka, S.; Sakamoto, R.; Kitagawa, Y.; Okumura, M.; Nishihara, H. An extremely bright heteroleptic bis(dipyrrinato)zinc(II) complex. *Chem. Asian J.* **2012**, *7*, 907–910, doi:10.1002/asia.201200131.
22. Kim, J.H.; Kim, H.S. Compensation Film and Organic Dot and Compensation Film. U.S. Patent 15,033,476, 7 May 2015.
23. Ramos-Torres, A.; Avellanal-Zaballa, E.; Prieto-Castañeda, A.; García-Garrido, F.; Bañuelos, J.; Agarrabeitia, A.R.; Ortiz, M.J. FormylBODIPYs by PCC-promoted selective oxidation of α-methylBODIPYs. Synthethic versatility and applications. *Org. Lett*. **2019**, *21*, 4563–4566, doi:10.1021/acsorglett.9b01465.